

# *Supplement of*

**Air Quality Index (AQI) Did Not Improve during the COVID-19 Lockdown in Shanghai, China, in 2022, Based on Ground and TROPOMI Observations**

Qihan Ma<sup>1</sup>, Jianbo Wang<sup>1</sup>, Ming Xiong<sup>2</sup>, Liye Zhu<sup>1,3,4\*</sup>

<sup>1</sup> *School of Atmospheric Sciences, Sun Yat-Sen University, Zhuhai 519082, China*

<sup>2</sup> *School of Computer Science and Engineering, Sun Yat-Sen University, Guangzhou 510006, China*

<sup>3</sup> *Southern Marine Science and Engineering Guangdong Laboratory (Zhuhai), Zhuhai 519082, China*

<sup>4</sup> *Key Laboratory of Tropical Atmosphere-Ocean System, Ministry of Education, Zhuhai 519082, China*

\* Correspondence: zhuly37@mail.sysu.edu.cn

## Content

Text S1-S4

Figures S1-S8

Tables S1-S6

References

### Text S1. The definition of the Air Quality Index (AQI)

Different countries may have different definitions of AQI, corresponding to the specific national air quality standards. The AQI used in this study refers to the AQI standard in China [1, 2].

The AQI levels are based on the concentrations of six air pollutants, including SO<sub>2</sub>, NO<sub>2</sub>, PM<sub>10</sub>, PM<sub>2.5</sub>, O<sub>3</sub>, and CO. To obtain the AQI, we first need to calculate the Individual Air Quality Index (IAQI). The IAQI is calculated using the breakpoint concentrations as shown in Table S7. The IAQI value is calculated as follows:

$$IAQI_p = \frac{IAQI_{Hi} - IAQI_{Lo}}{BP_{Hi} - BP_{Lo}}(C_p - BP_{Lo}) + IAQI_{Lo} \quad (S1)$$

Where  $IAQI_p$  is the  $IAQI$  of pollutant  $P$ ,  $C_p$  is the mass concentration of pollutant  $P$ . As shown in Table S7,  $BP_{Hi}$  is the higher threshold and  $BP_{Lo}$  is the lower threshold of pollutant concentration near  $C_p$ ,  $IAQI_{Hi}$  is the  $IAQI$  corresponding to  $BP_{Hi}$ , and  $IAQI_{Lo}$  is the  $IAQI$  corresponding to  $BP_{Lo}$ . The final daily AQI value is the highest of these values:

$$AQI = \max \{IAQI_1, IAQI_2, IAQI_3, \dots, IAQI_n\} \quad (S2)$$

In brief, AQI is the highest value of IAQIs. Subsequently, we can refer to Table S8 for the category of specific AQI values and the corresponding air pollution levels.

#### **Text S2. HCHO/NO<sub>2</sub> (FNR)**

For a better understanding of the ozone-NO<sub>x</sub>-VOCs relationships, we mostly need to measure NO<sub>x</sub>, VOCs, and their chemical reactivity or set well-established chemical transport models, which are limited to spatially sparse observations or large uncertainties [3-5]. To address the limitations, Sillman [6] first analyzed the chemical sensitivity of ozone production by using the concentration ratio of chemical proxies HCHO and NO<sub>y</sub>. As an extension of the study of Sillman [6], Martin et al. [7] made an early attempt to apply space-based measurements of tropospheric HCHO and NO<sub>2</sub> columns from the Global Ozone Monitoring Experiment (GOME) satellite instrument, which shows that HCHO/NO<sub>2</sub> (FNR) is an indicator of the relative sensitivity of surface ozone to emissions of NO<sub>x</sub> and VOCs.

#### **Text S3. Wilcoxon Signed Rank Test**

Wilcoxon Signed Rank Test is an improvement of the sign test method in nonparametric statistics, which not only uses the positive and negative difference between the observed value and the null hypothesis center position but also uses the information of the size of the difference value [8]. Although it is a simple nonparametric method, it embodies the basic idea of rank. The Wilcoxon Signed Rank Test can be utilized to determine whether the overall distribution of the corresponding data is the same without assuming that the data are normally distributed [8]. If the differences between data pairs are not normally distributed, Wilcoxon Signed Rank Test should be used.

#### **Text S4. The validation and quality of NO<sub>2</sub> and HCHO tropospheric VCDs data**

In terms of the validation of TROPOMI NO<sub>2</sub> and HCHO tropospheric VCDs data, for NO<sub>2</sub>, Wang et al. [9] found that TROPOMI tropospheric NO<sub>2</sub> VCDs closely match the MAX-DOAS records, since the correlation coefficients are above 0.8 and 0.95 for daily and monthly in China. Verhoelst et al. [10] demonstrated the TROPOMI NO<sub>2</sub> column data are in good geophysical and quantitative agreement with ground-based correlative data of documented quality and can be used for a variety of applications. Griffin et al. [11] showed that TROPOMI NO<sub>2</sub> VCDs product displays a high correlation with aircraft-borne and surface in-situ NO<sub>2</sub> observations and ground-based remote-sensing measurements over the Canadian Oil Sands.

For HCHO, Vigouroux et al. [12] demonstrated the very good quality of the TROPOMI HCHO products, which were well within the pre-launch requirements for both accuracy and precision by using ground-based solar-absorption FTIR (Fourier-transform infrared) measurements from 25 stations around the world. Chan et al. [13] showed that monthly averaged tropospheric HCHO VCDs derived from the MAX-DOAS measurements show a good correlation with TROPOMI observations in Munich.

The qa\_value, as the main quality indicator, indicates whether the footprint is cloud covered or not, and whether there is snow or ice on the surface [14, 15]. The threshold widely used is “qa\_value > 0.75” or “qa\_value > 0.5”. Their influences are as follows:

- qa\_value > 0.75.

This removes cloud-covered scenes (cloud radiance fraction > 0.5), part of the scenes covered by snow/ice, errors, and problematic retrievals [14].

- qa\_value > 0.50.

This adds good quality retrievals over clouds and over scenes covered by snow/ice. Errors and problematic retrievals are still filtered out [14].

In our study, compared to snow/ice on the surface, the data quality of tropospheric NO<sub>2</sub> VCDs over Shanghai during P1 to P4 was mainly affected by cloud-covered scenes. The pixel filters, including qa\_value > 0.5 and cloud radiation fraction > 0.5 are sufficient to ensure the data quality of NO<sub>2</sub> VCDs.

Excluding the default in Shanghai regions for some days due to fliriting or shortage of data, the typical number of pixels in each grid (i, j) for daily averaged NO<sub>2</sub> and HCHO VCDs is from 2 to 5.

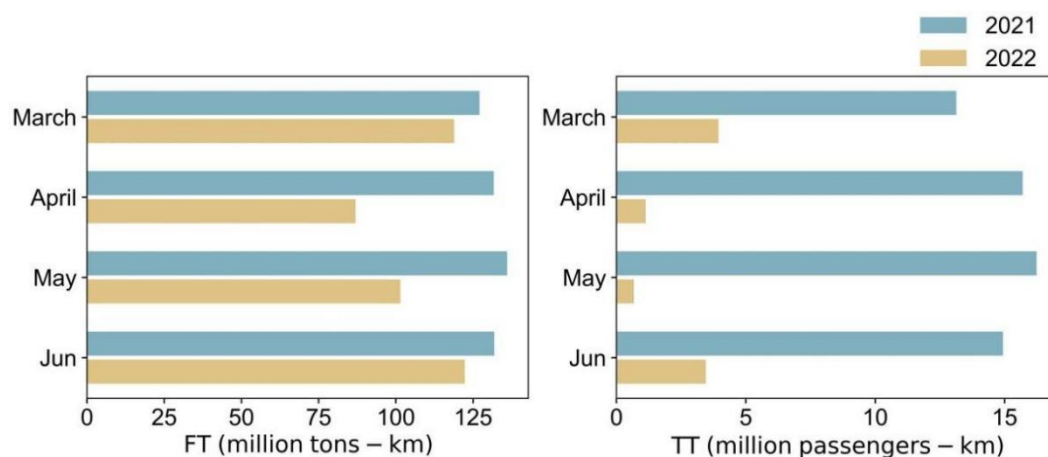


**Figure S1.** Monthly variations in freight turnover (FT) and tourist turnover (TT) in Shanghai from March to June in 2021 and 2022 (Note: FT refers to the amount of cargo transported in the compound unit of weight (in tons) and transport distance (in km) that is completed by various transport within a certain time. TT is the product of the number of passengers transported (in million passengers) and the transport distance (in km). Monthly FT and TT data were obtained from the Shanghai Municipal Bureau of Statistics (<http://tjj.sh.gov.cn/sjfb/index.html>, last accessed: November 11, 2022), including railway, highway, harbor, and civil aviation).

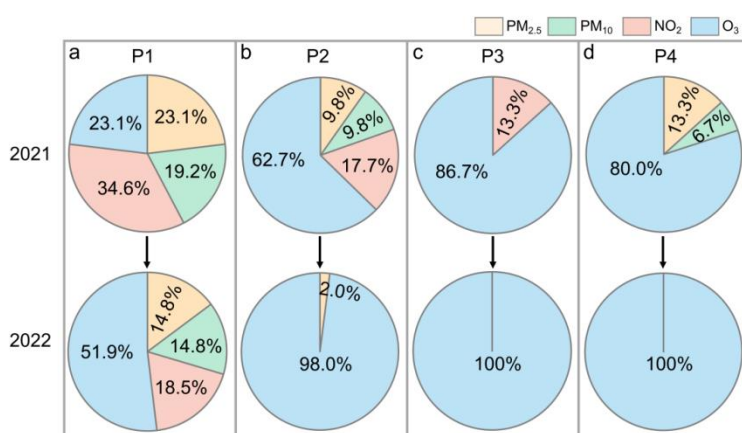


**Figure S2.** The occurrence frequency of dominant pollutants in Shanghai from P1 to P4 (a-d) in 2021 and 2022.

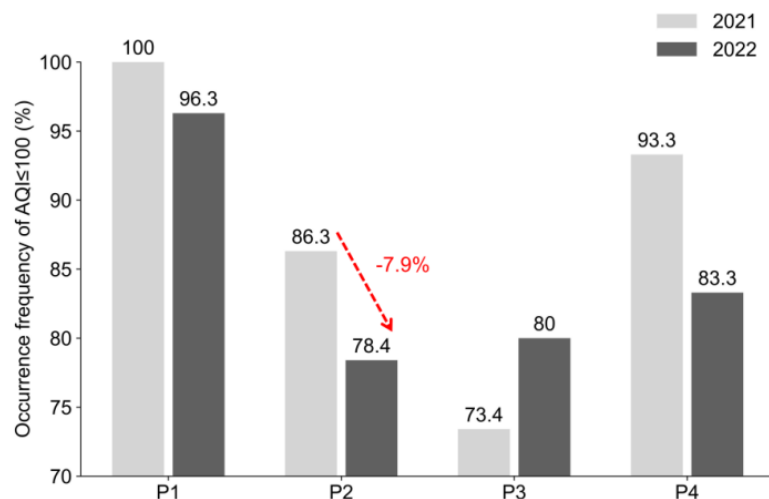


**Figure S3.** The occurrence frequency of  $AQI \leq 100$  (good or excellent air quality) from P1 to P4 in 2021 and 2022; the red arrow and value represent the absolute change during P2.

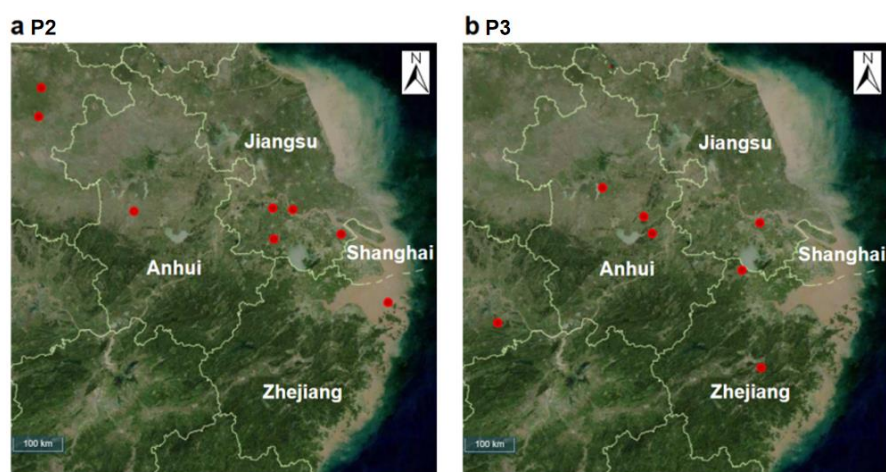


**Figure S4.** The distributions of fire spots caused by biomass burning detected from the Landsat-8 satellite (<http://satsee.radi.ac.cn:8080/index.html>) during P2 and P3 of 2022. The red dots represent fire spots caused by biomass burning.

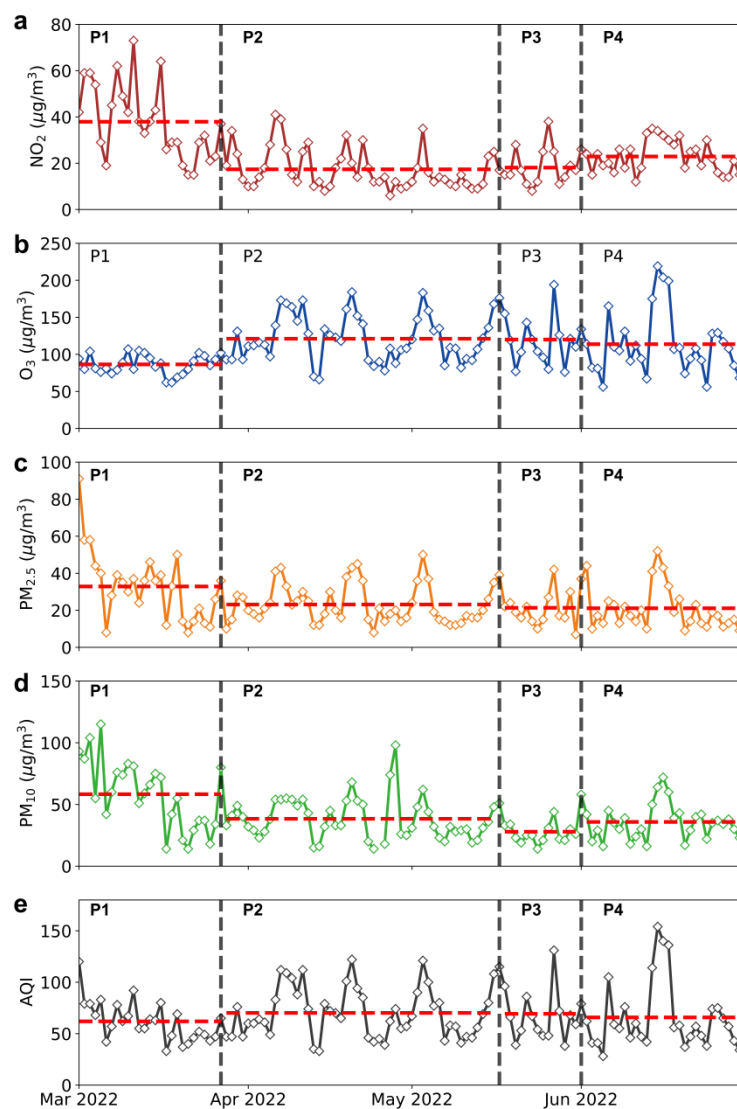


**Figure S5.** Time series of daily average  $\text{NO}_2$ ,  $\text{PM}_{2.5}$ ,  $\text{PM}_{10}$  concentrations, daily MDA8  $\text{O}_3$  concentrations, and daily AQI based on in-situ measurements over BS from P1 to P4 in 2022; The dashed red line indicates the mean value in each period.

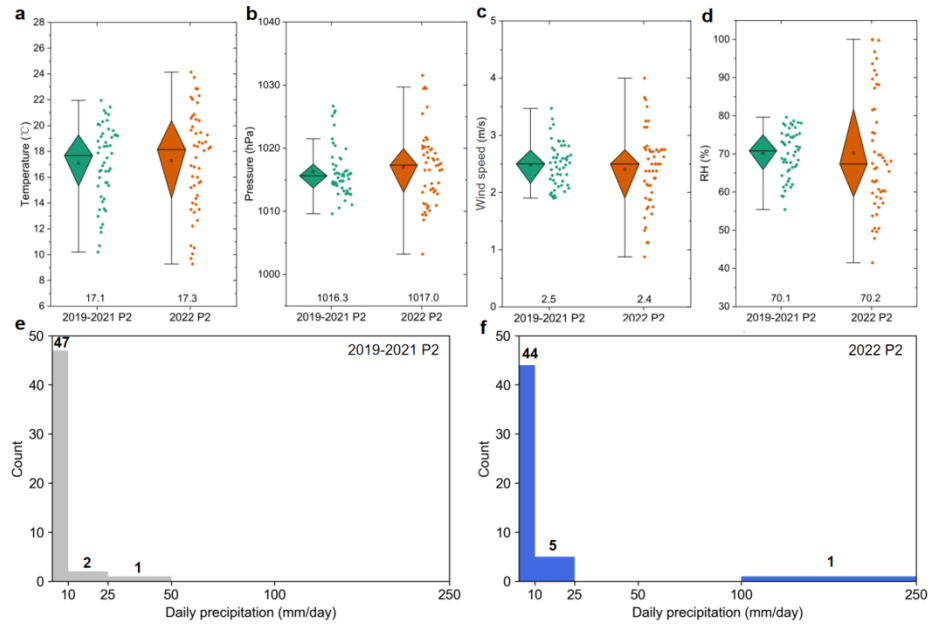


**Figure S6.** Daily temperature (a), pressure (b), wind speed (c), RH (d) during P2 of 2019-2021 and 2022 over BS. The average values were presented at the bottom. The horizontal bar and rectangle inside the box present the median line and the mean value, respectively. (e-f) Frequency distributions of daily precipitation during P2 of 2019-2021 and 2022 over BS.

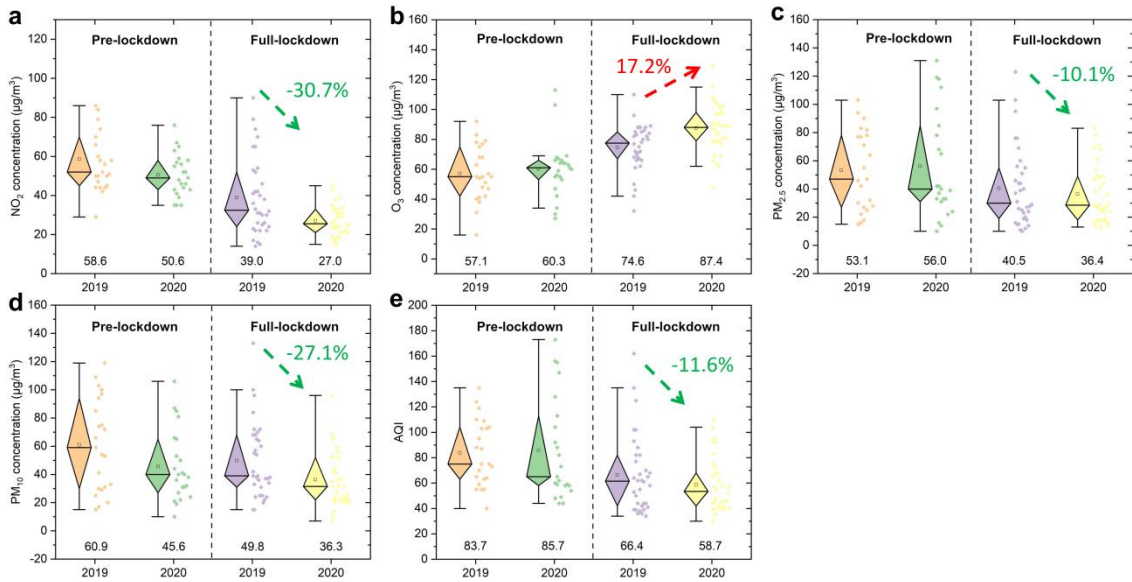


**Figure S7.** Daily air pollutants concentrations and AQI during pre-lockdown and full lockdown in 2019 and 2020 over Shanghai. The average values during each period were presented at the bottom (Note: the pre-lockdown and full-lockdown periods were divided according to Tanvir et al. [16]; the pre-lockdown period in 2020 is from January 1 to January 23; the full-lockdown period in 2020 is from January 24 to February 26).

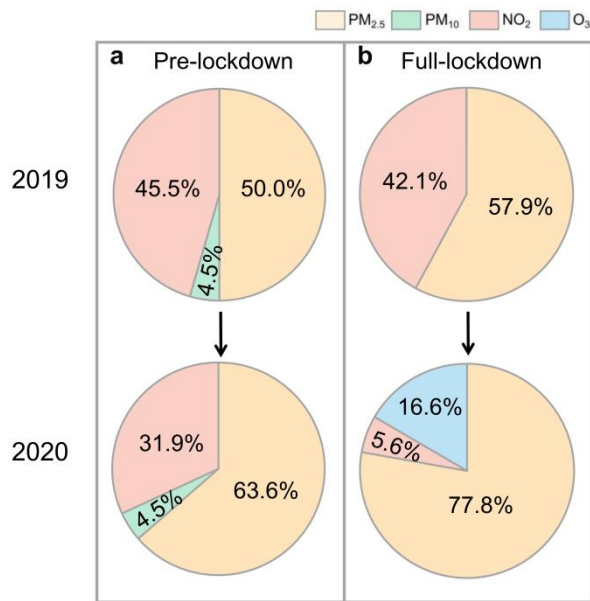


**Figure S8.** The occurrence frequency of dominant pollutants in Shanghai during pre-lockdown and full-lockdown in 2019 and 2020.

**Table S1.** Summary of observed data used in this study.

data	source	Resolution	Period
AQI, PM <sub>2.5</sub> , PM <sub>10</sub> , NO <sub>2</sub> , and MDA8 O <sub>3</sub>	Shanghai Municipal Ecological Environment Bureau	Shanghai, Daily	P1 to P4 in 2019-2022
		BS, Daily	P1 to P4 in 2019-2022
Dominant Pollutant	Shanghai Municipal Ecological Environment Bureau	Shanghai, Daily	P1 to P4 in 2019-2022
Air Temperature			
Atmospheric Pressure	National Data Center	Climatic BS (station index number: 58362), 3h	P2 in 2019-2022
Wind Speed			
RH	UK Meteorological Office	BS (station index number: 58362), 3h	P2 in 2019-2022
Precipitation		BS (station index number: 58362), 6h or 12h	

**Table S2.** Normal distribution test for different air pollutants and AQI from P1 to P4 using the Shapiro-Wilk test.

		P1	P2	P3	P4
NO <sub>2</sub>	2021	0.591	0.727	0.369	0.026*
	2022	0.530	<0.001*	0.658	0.240
O <sub>3</sub>	2021	0.019*	0.475	0.350	0.006*
	2022	0.507	0.159	0.241	0.116
PM <sub>2.5</sub>	2021	0.115	<0.001*	0.109	0.016*
	2022	0.018*	<0.001*	0.198	0.008*
PM <sub>10</sub>	2021	0.032*	<0.001*	0.074	0.062
	2022	0.660	0.024*	0.085	0.230
AQI	2021	0.282	<0.001*	0.130	<0.001*
	2022	0.192	0.036*	0.117	0.009*

**Note:** The values present the Shapiro-Wilk P; if  $P \ll 0.05$ , the data were not normally distributed (shown with "\*\*\*").

**Table S3.** The variance inflation factor (VIF) of different meteorology predictors

	Temperature	Pressure	Wind Speed	RH	Precipitation
VIF	3.123	3.765	1.013	1.666	1.216

**Table S4.** The stepwise MLR regression results of NO<sub>2</sub>, O<sub>3</sub>, PM<sub>2.5</sub>, and PM<sub>10</sub> during the full lockdown in the case study of BS.  $\beta_k$  is the repression coefficient for the k-th meteorological variable.

		NO <sub>2</sub>	O <sub>3</sub>	PM <sub>2.5</sub>	PM <sub>10</sub>
Temperature (°C)		0.903**	+3.276***	–	1.657***
Pressure (hPa)		–	–	-1.076***	-
Wind Speed (m/s)	$\beta_k$	-8.671***	–	-4.043*	–
RH (%)		-0.210**	-1.381***	–	-0.694***
Precipitation (mm/day)		–	–	-0.620*	-0.509*
Intercept ( $\beta_0$ )		66.840***	147.343***	1139.351***	66.090***
Adjust R <sup>2</sup>		0.3	0.5	0.2	0.4
p		<0.001	<0.001	<0.001	<0.001

**Note:** for k-th meteorological variable, \*\*\*:  $p < 0.001$ , \*\*:  $p < 0.01$ , and \*:  $p < 0.05$ .

**Table S5.** Daily air pollutant concentrations and AQI from P1 to P4 in 2022 in Shanghai compared with the same periods in 2021 by the Wilcoxon Signed Rank Test.

	P1	P2	P3	P4
NO <sub>2</sub>	-2.091*	-5.925**	-3.411**	-4.296**
O <sub>3</sub>	-3.213**	-3.051**	-0.114	-2.304*
PM <sub>2.5</sub>	-0.949	-2.651**	-2.294*	-0.617
PM <sub>10</sub>	-1.177	-2.694**	-1.335	-0.671
AQI	-0.361	-0.845	<0.001	-1.831

**Note:** \*p < 0.05 means a significant difference and \*\*p < 0.01 means a highly significant difference; the higher the absolute value, the greater the variation.

**Table S6.** Concentration limits of basic ambient air pollutants according to the Environmental Air Quality Standard of China (GB3095-2012) [1].

Ambient air pollutants	Average time	Concentration limits (µg/m <sup>3</sup> )	
		Level I	Level II
NO <sub>2</sub>	Annual mean	40	40
	24-hour mean	80	80
	1-hour mean	200	200
PM <sub>2.5</sub>	Annual mean	15	35
	24-hour mean	35	75
PM <sub>10</sub>	Annual mean	40	70
	24-hour mean	50	150
O <sub>3</sub>	Daily maximum 8-hour mean	100	160
	1-hour mean	160	200

**Table S7.** Chinese AQI Category and pollutant breakpoints [2].

Individual index	Units are $\mu\text{g}/\text{m}^3$ except for CO, which is $\text{mg}/\text{m}^3$									
	SO <sub>2</sub> 24-hour mean	SO <sub>2</sub> 1-hour mean (1)	NO <sub>2</sub> 24-hour mean	NO <sub>2</sub> 1-hour mean (1)	PM <sub>10</sub> 24-hour mean	CO 24-hour mean	CO 1-hour mean (1)	O <sub>3</sub> 1-hour mean	O <sub>3</sub> 8-hour moving average	PM <sub>2.5</sub> 24-hour mean
0	0	0	0	0	0	0	0	0	0	0
50	50	150	40	100	50	2	5	160	100	35
100	150	500	80	200	150	4	10	200	160	75
150	475	650	180	700	250	14	35	300	215	115
200	800	800	280	1200	350	24	60	400	265	150
300	1600	(2)	565	2340	420	36	90	800	800	250
400	2100	(2)	750	3090	500	48	120	1000	(3)	350
500	2620	(2)	940	3840	600	60	150	1200	(3)	500

**Notes:**

(1) The SO<sub>2</sub>, NO<sub>2</sub>, and CO 1-hour averaged concentrations are only for real-time reporting. For daily reports, the 24-hour averaged concentrations should be used.

(2) If the SO<sub>2</sub> 1-hour averaged concentrations exceed 800  $\mu\text{g}/\text{m}^3$ , the index of the 24-hour averaged concentrations should be used.

(3) If the concentrations of O<sub>3</sub> 8-hour moving average exceed 800  $\mu\text{g}/\text{m}^3$ , the index of the 1-hour averaged concentrations should be used.

**Table S8.** Air pollution level and category according to AQI [2].

AQI	Air Pollution Level	Air Pollution Category
0–50	Level 1	Excellent
51–100	Level 2	Good
101–150	Level 3	Lightly Polluted
151–200	Level 4	Moderately Polluted
201–300	Level 5	Heavily Polluted
>300	Level 6	Severely Polluted

## References

1. Ministry of Ecology and Environment of the People's Republic of China. Ambient air quality standards. Available online: <https://www.mee.gov.cn/ywgz/fgbz/bz/bzwb/dqhjbh/dqhjzlbz/> (accessed on 11 December 2022).
2. Ministry of Ecology and Environment of the People's Republic of China. Technical Regulation on Ambient Air Quality Index (on trial). Available online: <https://www.mee.gov.cn/ywgz/fgbz/bz/bzwb/jcffbz/> (accessed on 11 December 2022).
3. Choi, Y.; Souri, A.H. Chemical condition and surface ozone in large cities of Texas during the last decade: Observational evidence from OMI, CAMS, and model analysis. *Remote Sens. Environ.* **2015**, *168*, 90–101.
4. Souri, A.H.; Nowlan, C.R.; Wolfe, G.M.; Lamsal, L.N.; Chan Miller, C.E.; Abad, G.G.; Janz, S.J.; Fried, A.; Blake, D.R.; Weinheimer, A.J.; *et al.*. Revisiting the effectiveness of HCHO/NO<sub>2</sub> ratios for inferring ozone sensitivity to its precursors using high resolution airborne remote sensing observations in a high ozone episode during the KORUS-AQ campaign. *Atmos. Environ.* **2020**, *224*, 117341.
5. Sillman, S. The relation between ozone, NO<sub>x</sub> and hydrocarbons in urban and polluted rural environments. *Atmos. Environ.* **1999**, *33*, 1821–45.
6. Sillman, S. The use of NO<sub>y</sub>, H<sub>2</sub>O<sub>2</sub>, and HNO<sub>3</sub> as indicators for ozone-NO<sub>x</sub>-hydrocarbon sensitivity in urban locations. *J. Geophys. Res. Atmos.* **1995**, *100*, 14175–88.
7. Martin, R.V.; Fiore, A.M.; Van Donkelaar, A. Space-based diagnosis of surface ozone sensitivity to anthropogenic emissions. *Geophys. Res. Lett.* **2004**, *31*, L6120.
8. Wilcoxon, F. Individual Comparisons by Ranking Methods. *Biometrics.* **1945**, *1*, 196–202.
9. Wang, C.; Wang, T.; Wang, P.; Rakitin, V. Comparison and Validation of TROPOMI and OMI NO<sub>2</sub> Observations over China. *Atmosphere* **2020**, *11*, 636.
10. Verhoelst, T.; Compernolle, S.; Pinardi, G.; Lambert, J.; Eskes, H.J.; Eichmann, K.; Fjæraa, A.M.; Granville, J.; Niemeijer, S.; Cede, A.; *et al.*. Ground-based validation of the Copernicus Sentinel-5P TROPOMI NO<sub>2</sub> measurements with the NDACC ZSL-DOAS, MAX-DOAS and Pandonia global networks. *Atmos. Meas. Tech.* **2021**, *14*, 481–510.
11. Griffin, D.; Zhao, X.; McLinden, C.A.; Boersma, F.; Bourassa, A.; Dammers, E.; Degenstein, D.; Eskes, H.; Fehr, L.; Fioletov, V.; *et al.*. High-Resolution Mapping of Nitrogen Dioxide With TROPOMI: First Results and Validation Over the Canadian Oil Sands. *Geophys. Res. Lett.* **2019**, *46*, 1049–60.
12. Vigouroux, C.; Langerock, B.; Bauer Aquino, C.A.; Blumenstock, T.; Cheng, Z.; De Mazière, M.; De Smedt, I.; Grutter, M.; Hannigan, J.W.; Jones, N.; *et al.*. TROPOMI–Sentinel-5 Precursor formaldehyde validation using an extensive network of ground-based Fourier-transform infrared stations. *Atmos. Meas. Tech.* **2020**, *13*, 3751–67.
13. Chan, K.L.; Wiegner, M.; van Geffen, J.; De Smedt, I.; Alberti, C.; Cheng, Z.; Ye, S.; Wenig, M. MAX-DOAS measurements of tropospheric NO<sub>2</sub> and HCHO in Munich and the comparison to OMI and TROPOMI satellite observations. *Atmos. Meas. Tech.* **2020**, *13*, 4499–520.
14. Eskes, H.; van Geffen, J.; Boersma, F.; Eichmann, K.; Apituley, A.; Pedernana, M.; Sneep, M.; Veefkind, J.P.; Loyola, D. Sentinel-5 precursor/TROPOMI Level 2 Product User Manual Nitrogen dioxide. Available online: <https://sentinel.esa.int/documents/247904/3541451/Sentinel-5P-Nitrogen-Dioxide-Level-2-Product-Readme-File> (accessed on 11 December 2022).
15. Romahn, F.; Pedernana, M.; Loyola, D.; Apituley, A.; Sneep, M.; Veefkind, J.P.; De Smedt, I.; Chan, K.L. Sentinel-5 precursor/TROPOMI Level 2 Product User Manual Formaldehyde HCHO. Available

online: <https://sentinel.esa.int/documents/247904/3541451/Sentinel-5P-Formaldehyde-Readme.pdf>  
(accessed on 11 December 2022).

16. Tanvir, A.; Javed, Z.; Jian, Z.; Zhang, S.; Bilal, M.; Xue, R.; Wang, S.; Bin, Z. Ground-Based MAX-DOAS Observations of Tropospheric NO<sub>2</sub> and HCHO During COVID-19 Lockdown and Spring Festival Over Shanghai, China. *Remote Sens.* **2021**, *13*, 488.